第 6 卷　第 1 期
2017 年 1 月

集　　成　　技　　术
JOURNAL OF INTEGRATION TECHNOLOGY

Vol. 6　No. 1
Jan. 2017

施加偏压对采用等离子体辅助热丝化学气相沉积法在硬质合金上沉积金刚石 / 碳化硅 / 硅化钴复合薄膜的影响

王　陶　蒋春磊　唐永炳

（中国科学院深圳先进技术研究院 功能薄膜中心　深圳　518055）

摘　要　金刚石涂层硬质合金是一种出众的刀具材料，将碳化硅掺入金刚石涂层中不仅可以提高涂层的断裂韧性，还能够提高薄膜与基体之间的粘附性。文章采用氢气、甲烷和四甲基硅烷混合气体作为反应气体，用直流等离子体辅助热丝化学气相沉积法在硬质合金基体上沉积金刚石-碳化硅-硅化钴复合薄膜。通过扫描电子显微镜、电子探针显微分析、X 射线衍射和拉曼光谱对薄膜的表面形貌、成分以及结构进行了分析，结果显示此复合薄膜中含有金刚石、碳化硅（β-SiC）和硅化钴（Co_2Si、CoSi）。复合薄膜的结构和成分可通过调节偏流和气相中四甲基硅烷的浓度来控制，随着偏流的增加，复合薄膜中金刚石晶粒尺寸变大且含量增加，β-SiC 的含量减少，因为复合薄膜沉积过程中正偏压促进金刚石的生长，并且增强金刚石的二次形核。虽然电子轰击同时增强了氢气、甲烷和四甲基硅烷的分解，但随着偏流的增加，气相中产生的碳源浓度高于硅源浓度，使金刚石比 β-SiC 在空间生长上更具有优势。当偏流过高时则形成纯金刚石，不能够同时沉积金刚石、β-SiC 和硅化钴三种物质。通过调节偏压和气体成分，金刚石和碳化硅在复合薄膜中的分布得以控制。该工作有助于理解和控制复合材料和超硬薄膜的生长，所产生的复合薄膜可用于提高金刚石涂层刀具切削性能。

关键词　金刚石/碳化硅/硅化钴复合薄膜；偏压；金刚石；硬质合金；热丝化学气相沉积

中图分类号　TG 156　**文献标志码**　A

Effect of Bias on Deposition of Diamond/β-SiC/Cobalt Silicide Composite Films on Cemented Carbide Substrates by Plasma Assisted Hot Filament Chemical Vapor Deposition

WANG Tao　JIANG Chunlei　TANG Yongbing

(*Functional Thin Films Research Center, Shenzhen Institutes of Advanced Technology, Chinese Academy of Sciences,*
Shenzhen 518055, *China*)

Abstract　Diamond coated hard metal is an outstanding cutting material for manufacturing. By adding

---

收稿日期：2016-10-13　**修回日期**：2016-11-29

基金项目：广东省创新团队项目（2013C090）；广东省自然科学基金（2014A030310482）；深圳市科技计划项目（JCYJ20160122143155757）；中国科学院科研设备项目（yz201440）

作者简介：王陶，博士，研究方向为金刚石薄膜的制备及应用；蒋春磊，博士，研究方向为金刚石薄膜的制备及应用；唐永炳（通讯作者），博士，研究员，研究方向为硬质与超硬涂层，E-mail：tangyb@siat.ac.cn。

SiC to the diamond coating material, not only the surface toughness but also the film adhesive strength can be improved. Diamond/β-SiC/cobalt silicide composite films were deposited on Co-cemented tungsten carbide (WC-Co) substrates by direct current plasma assisted hot filament chemical vapor deposition using a gas mixture of hydrogen, methane and tetramethylsilane. Scanning electron microscopy, electron probe microanalysis, X-ray diffraction and Raman scattering analyses were carried out to characterize the surface morphology, composition and structure of the deposited films. The results revealed that the composite films consist of diamond, β-SiC and cobalt silicides (Co_2Si, CoSi). The structure and composition of the composite films can be controlled by adjusting bias current and tetramethylsilane concentration in the gas phase. With the increase of bias current, the grain size and content of diamond also increase, while the content of β-SiC decrease. Since bias current enhances the secondary nucleation and growth of diamond. Although the dissociation of hydrogen, methane and tetramethylsilane are all enhanced by electron bombardment during the biasing process, the concentration of produced C sources is much higher than that of Si sources with the increase of bias current. Then the growth of diamond becomes more competitive than that of β-SiC. The bias current cannot be too high to deposit the three substances of diamond, β-SiC and cobalt silicides. By adjusting bias and gas composition, the distribution of diamond and β-SiC in the composite films was manipulated. These results demonstrated the significance to understand and control the growth of composite materials and super hard thin films. Such composite films can be utilized to improve the cutting performance of diamond coated cutting tools.

Keywords　thin film; bias; diamond; cemented carbide substrate; hot filament chemical vapor deposition

1　Introduction

Diamond possesses many unique properties including high hardness, low friction coefficient and high wear resistance. The performances of cemented carbide (WC-Co) tools coated with chemical vapor deposition diamond films can be greatly improved during cutting or milling operations on non-ferrous materials. However, it has been proven difficult to deposit well-adherent diamond films on WC-Co tools[1-5]. The major reason is the strong catalytic effect of cobalt contained in WC-Co substrate, which preferentially promotes the formation of feeble graphite[6]. Moreover, the high thermal stresses caused by the mismatch in the expansion coefficient between diamond coating and WC-Co substrate are formed in the diamond film at the substrate edges during the cooling down process after deposition[7]. Thus, substrate pretreatments or interlayers have been applied to solve these problems[8,9].

A good interlayer system should not only have a low diffusion coefficient for both C and Co, but also possess a low thermal expansion coefficient to reduce the residual stress at the interface. Keeping the above aspects in mind, different interlayer systems, such as TiN, TiC, SiC, CrN, Si_3N_4, have been deposited onto the WC-Co substrate using either physical vapor deposition or chemical vapor deposition techniques[10,11]. However, the results are still far away from satisfactory because of low diamond nucleation density on these interfaces, which leads to a very low growth rate of the diamond layer[12,13]. In addition to the above issue, the poor adhesion of diamond films also results from the high residual stress at the interface[13-15], particularly around a cutting edge[16], which requires a special research attention.

Comparing with other interlayer systems, a gradient composite interlayer with diamond as one of the components is an effective way to enhance the adhesion of diamond films. Because such interlayer manipulates the thermally induced shear stress distribution over the composite interlayer and reduces the shear stress maximum/peak value[17-19]. The thermal stress induced in the film could be further reduced by manipulating the distribution of diamond and β-SiC in the composite film[19,20]. However, few studies have been done on the study of understanding and controlling the distribution of diamond and β-SiC phases in the film. To the best of our knowledge, this is the first work that investigates the effect of bias on the growth process of diamond/β-SiC films. The application of bias to the substrate (with respect to the filament) affects diamond nucleation and growth and their magnitude depends on bias amount as well as its polarity[21-24]. In this work, all the composite films were deposited by direct current (DC)-plasma assisted hot filament chemical vapor deposition (HFCVD) using hydrogen (H_2), methane (CH_4) and tetramethylsilane ($Si(CH_3)_4$, TMS) as reactive gases. The surface morphology, composition and structure of the deposited composite films were studied under different bias currents and various TMS concentrations. The structure and composition could finally be controlled by applying bias. The effects of bias on the growth of composite films were also discussed.

2 Experimental

The substrates used in this study were commercially available brazed cemented tungsten carbides YG6X (WC-6 wt% Co) inserts. Prior to deposition, the inserts were first immersed for 30 min in Murakami solution (10 g $K_3\left[Fe(CN)_6\right]$+10 g KOH+100 mL H_2O)[25] followed by a rinse in distilled water, and then immersed for 60 s in H_2SO_4 (30%)± H_2O_2 (70%) to remove cobalt from surface followed by a rinse in distilled water. Finally the inserts were ultrasonically seeded for 60 min with nanodiamond particles (size range 0 - 100 nm) suspended in water, followed by ultrasonically cleaning in ethanol.

Diamond/β-SiC/cobalt silicide composite films were deposited in a DC-plasma assisted HFCVD apparatus shown in Fig. 1. There are two separate power supplies. One is an alternating current power for filaments, and the other is a DC power for bias. The substrate was grounded and positively biased. The filaments were negative as opposed to the substrate. The diameter of the filaments was 0.6 mm. The distance between the filaments and the substrate was 8 mm. The filament temperature was 2 200℃, as measured by a two-colour infrared thermometer (Raytek MR1SC). The substrate temperature was kept at 800℃, which was measured with a W/Re thermocouple. At beginning of deposition, all samples were biased under the bias current of 1.5 A with 1.5 vol% CH_4 in H_2 for 30 min in order to enhance diamond nucleation. Then TMS was introduced into chamber for deposition of composite films. The total gas flow rate was kept at 206 sccm at a pressure of 1.5 kPa. The volume radio of CH_4 and H_2 is around 1%. The composite films were deposited with different bias currents under various TMS concentrations in gas phase of 0.075 vol%, 0.15 vol% and 0.175 vol%. The bias current was adjusted between 0 and 4.5 A. All the composite films were deposited for 7 h. The thickness of composite films is about 2 μm.

The whole set of samples is listed in Table 1.

Scanning electron microscopy (SEM, JSM-5600LV) was used to characterize the surface morphology of films. Energy dispersive X-ray spectroscopy was utilized to perform microanalysis in selected areas of the samples' surface. Electron probe microanalysis (EPMA-1600) was used to obtain the quantitative elemental composition with acceleration voltage of 15.0 kV and beam size of 10 μm. To determine the phase structure of films, X-ray diffraction experiments (XRD-6000, Cu Kα radiation, 40 kV and 30 mA) were performed in $\theta/2\theta$ geometry. Finally, Raman scattering (RENISHAW inVia Raman microscope) was carried out to identify diamond and non-diamond phases. The 632.8 nm line of a He-Ne laser was used as excitation source.

3　Results and discussion

Figs. 2-4 show the SEM surface morphologies of different diamond/β-SiC/cobalt silicide composite films deposited on WC-Co substrates. In Fig. 2, a series of composite films were synthesized at a constant TMS concentration of 0.075 vol% in gas phase with only a change in bias current. Fig. 2(a) shows the morphology of composite film deposited without bias (sample A1). The substrate appears to be covered with β-SiC clusters in nanometer size and a number of bigger (about 1 μm) particles. Even though XRD and Raman results (to be discussed) show diamond in this film. Energy dispersive X-ray spectroscopy spectra of the particles about 1 μm in size acquired in spot mode show the presence of Co and Si only Fig. 2(a). As XRD pattern shows Co_2Si and CoSi in the film (Fig. 6(a)), the particles about 1 μm

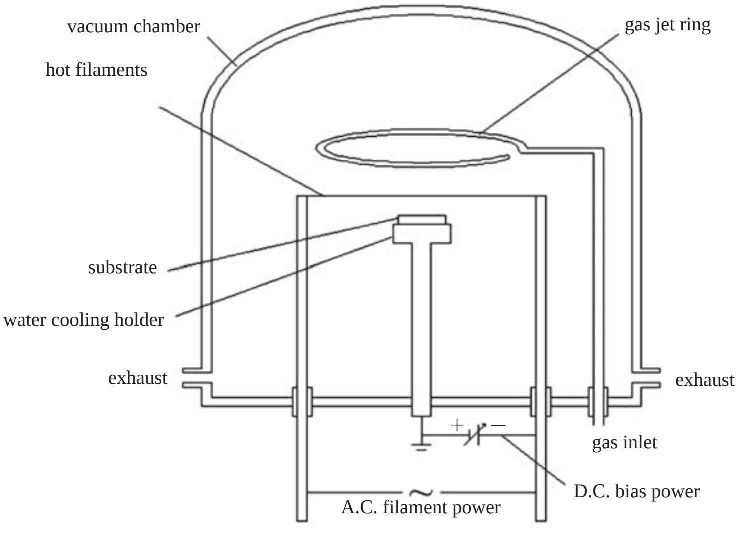

Fig. 1　Schematic diagram of DC-plasma assisted hot filament chemical vapor deposition apparatus

Table 1　List of diamond/β-SiC films deposited on cemented carbide substrates with different deposition parameters

Sample No.	A1	A2	A3	B1	B2	B3	C1	C2	C3
TMS in gas phase (vol%)	0.075	0.075	0.075	0.15	0.15	0.15	0.175	0.175	0.175
bias current (A)	0	1.5	3.0	1.5	3.0	4.5	1.5	3.0	4.5

in size correspond to Co_2Si and/or CoSi. Fig. 2(b) and 2(c) show the second electron image and the backscattered electron image of the composite film deposited with the bias current of 1.5 A (sample A2). As XRD and Raman results show diamond, β-SiC, Co_2Si and CoSi in this film, the dark, gray and white areas in Fig. 2(c) correspond to diamond, β-SiC and cobalt silicides (CoSi, Co_2Si), respectively. The grain sizes of diamond crystallites varied from 0.5 μm to 1 μm. The β-SiC crystallites are in nanometer size. The cobalt silicides particles are about 1 μm in size. Fig. 2(d) shows only diamond crystallites in the film deposited with bias current of 3.0 A (sample A3). Characteristic triangular faceted diamond crystallites from 0.5 μm to 2 μm in size can be observed throughout the surface. In short, with the increase of bias current, the grain size of diamond becomes larger, the content of diamond increased, while the content of β-SiC decreased.

Diamond/β-SiC/cobalt silicide composite films deposited with 0.15 vol% TMS and 0.175 vol% TMS with the increase of bias current reflect more or less the same nature as the films deposited with 0.075 vol% TMS discussed above. Fig. 3 shows the SEM surface morphologies of composite films deposited with 0.15 vol% TMS in the gas phase with only a change in bias current. Fig. 3(a) shows the morphology of composite film deposited with the bias current of 1.5 A (sample B1). It appears that the substrate is covered mostly by nanocrystalline β-SiC, though the XRD pattern shows diamond and cobalt silicides in the film. Figs. 3(b) and 3(c) show the second electron image and backscattered electron image of composite film deposited with the bias

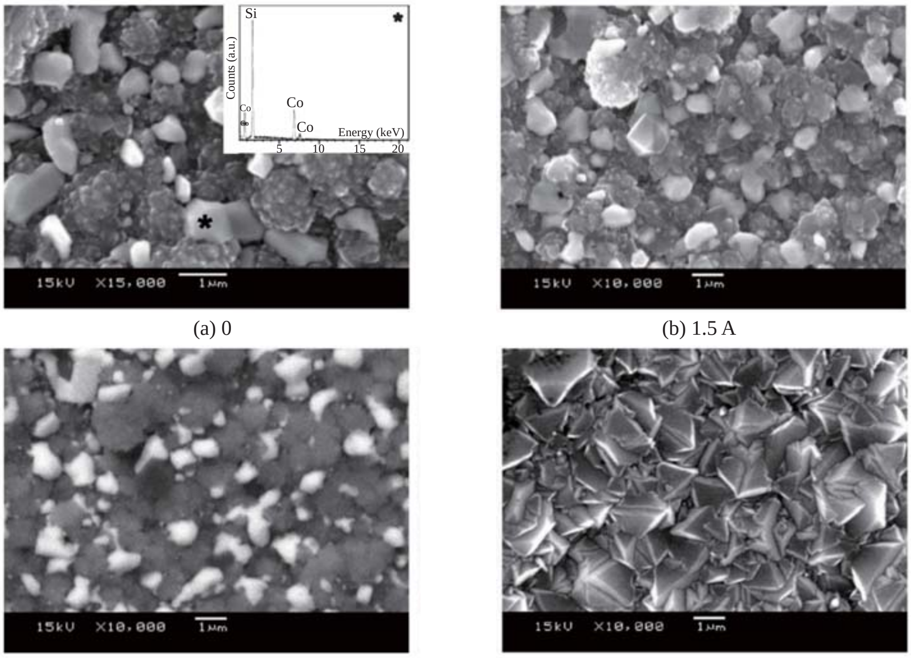

(a) 0

(b) 1.5 A

(c) 1.5 A

(d) 3.0 A

Fig. 2 Scanning electron micrographs of composite films deposited with 0.075 vol% tetramethylsilane in gas phase with bias currents of (a) 0 (sample A1), (b) 1.5 A (sample A2) and (d) 3.0 A (sample A3). Backscattered electron image of the composite film deposited with 1.5 A (sample A2) is shown in (c). The energy dispersive X-ray pectroscopy spectrum of particle with asterisk is shown in the insert

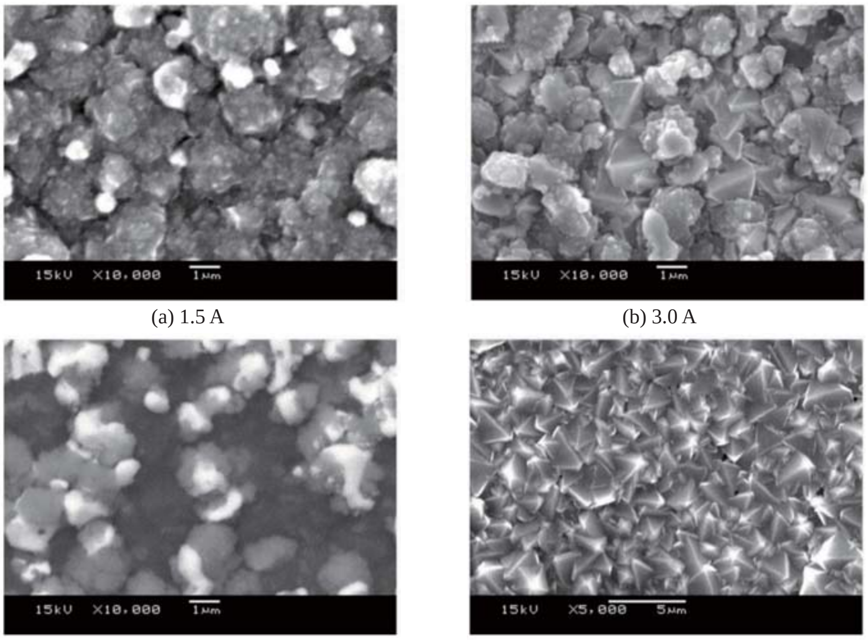

(a) 1.5 A (b) 3.0 A

(c) 3.0 A (d) 4.5 A

Fig. 3　Scanning electron micrographs of composite films deposited with 0.15 vol% tetramethylsilane in gas phase with bias currents of (a) 1.5 A (sample B1), (b) 3.0 A (sample B2) and (d) 4.5 A (sample B3). Backscattered electron image of the composite film deposited with 3.0 A (sample B2) is shown in (c)

current of 3.0 A (sample B2). In Fig. 3(c), there are three kinds of substances in different contrast. The dark, gray and white areas correspond to diamond, β-SiC and cobalt silicides respectively. It can be observed that diamond crystallites are around 1.5 μm in size, β-SiC grains are in nanometer size, and cobalt silicides are around 1 μm in irregular shape. Fig. 3(d) shows only diamond crystallites in the film deposited with the bias current of 4.5 A (sample B3).

Fig. 4 shows the SEM surface morphologies of diamond/β-SiC/cobalt silicide composite films deposited with 0.175 vol% TMS in the gas phase with only a change in bias current. Fig. 4(a) shows the morphology of composite film deposited with bias current of 1.5 A (sample C1). The substrate appears to be covered with β-SiC crystallites in nanometer size, though the XRD pattern shows diamond and Co_2Si in this film. Fig. 4(b) and 4(c) show the second electron image and backscattered electron image of composite film deposited with the bias current of 3.0 A (sample B2). In Fig. 4(c), dark areas correspond to diamond which are in micron size, and gray areas correspond to β-SiC which are in nanometer size. The bright particles in Fig. 4(c) indicate the existence of cobalt silicides about 0.5 μm in size. For the film deposited with bias current of 4.5 A, Fig. 4(d) indicates that the substrate is covered mostly by diamond crystallites.

EPMA of the diamond/β-SiC/cobalt silicide composite films grown on WC-Co substrates shows that there are only C, Si and Co elements in the films. Fig. 5 shows the variation of molar fraction of C, Si and Co in diamond/β-SiC/cobalt silicide composite films with bias currents. The variation trends of molar fraction of C and Si with bias current are similar with the films deposited with different TMS

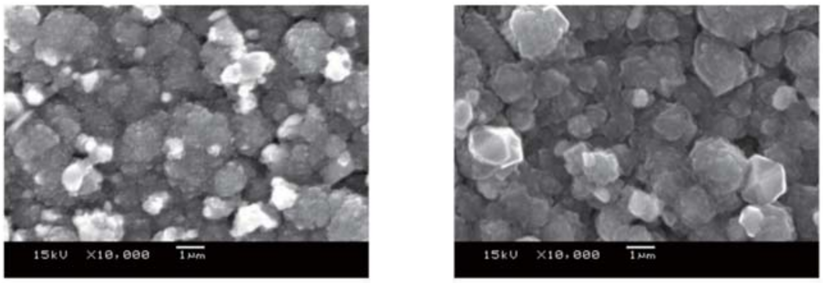

(a) 1.5 A (b) 3.0 A

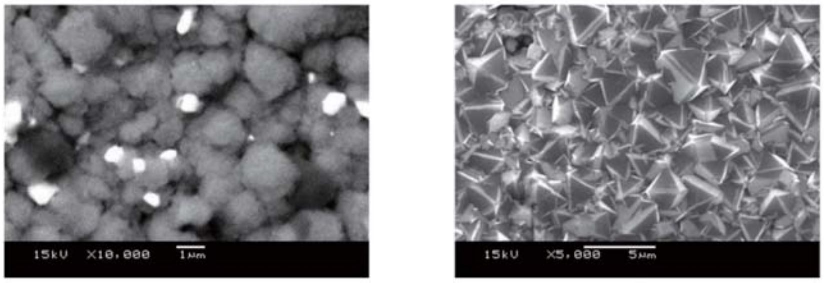

(c) 3.0 A (d) 4.5 A

Fig. 4 Scanning electron micrographs of composite films deposited with 0.175 vol% tetramethylsilane in gas phase with bias currents of（a）1.5 A（sample C1）,（b）3.0 A（sample C2）and（d）4.5 A（sample C3）. Backscattered electron image of the composite film deposited with 3.0 A（sample C2）is shown in（c）

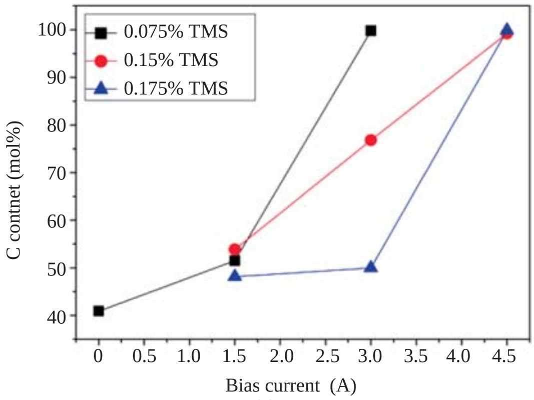

(a) C

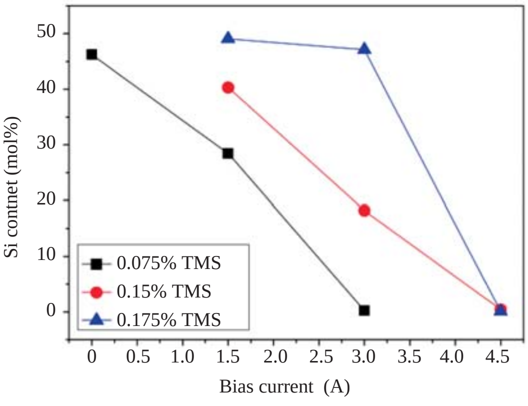

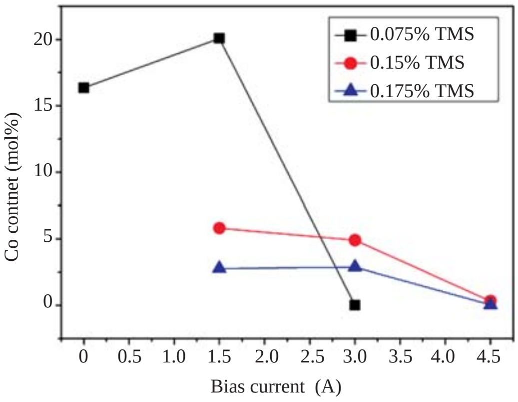

(b) Si (c) Co

Fig. 5 Electron probe microanalysis showing the variation of molar fraction (%) of (a) C, (b) Si and (c) Co with bias current

concentrations in the gas phase. With the increase of bias current from 0 to 4.5 A, the molar fraction of C increased as shown in Fig. 5(a), while that of Si decreased shown in Fig. 5(b). However, there is not a consistent trend for Co with the increase of bias current in Fig. 5(c).

Figs. 6-8 show the XRD patterns of the composite films deposited with different TMS concentrations in the gas phase and various bias currents. The results indicate that diamond, β-SiC and cobalt silicides (CoSi, Co_2Si) are deposited in the composite films with the appropriate TMS concentrations and bias currents. The intense WC peaks correspond to WC-Co substrate. Fig. 6 shows the XRD patterns of composite films deposited with 0.075 vol% TMS in the gas phase. The composite films deposited with bias currents of 0 and 1.5 A consist of diamond, β-SiC, Co_2Si and CoSi. The film deposited with

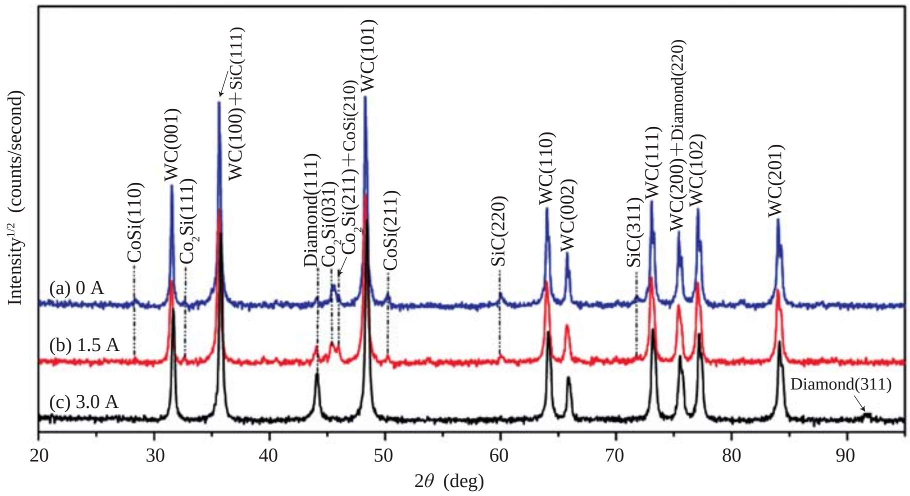

Fig. 6　X-ray diffraction patterns of composite films deposited with 0.075 vol% tetramethylsilane in the gas phase with bias currents of (a) 0 (sample A1), (b) 1.5 A (sample A2), and (c) 3.0 A (sample A3)

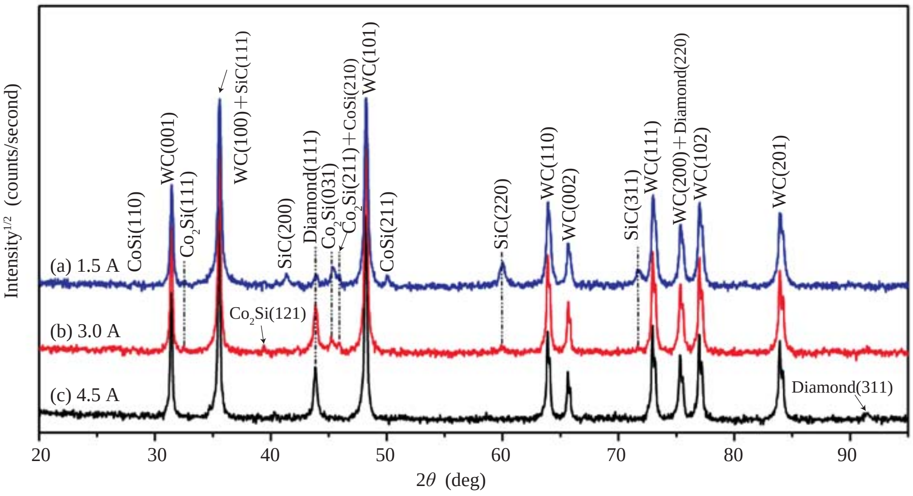

Fig. 7　X-ray diffraction patterns of composite films deposited with 0.15 vol% tetramethylsilane in the gas phase with bias currents of (a) 1.5 A (sample B1), (b) 3.0 A (sample B2), and (c) 4.5 A (sample B3)

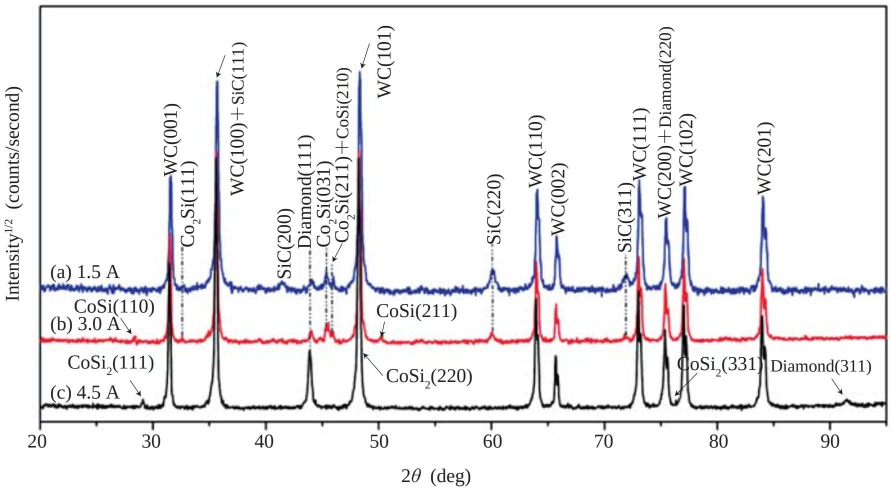

Fig. 8 X-ray diffraction patterns of composite films deposited with 0.175 vol% tetramethylsilane in the gas phase with bias currents of (a) 1.5 A (sample C1), (b) 3.0 A (sample C2), and (c) 4.5 A (sample C3)

bias current of 3.0 A contains only diamond. With the increase of bias current, the peak intensities corresponding to diamond increase, indicating the increase in its content in the films, while the peak intensities corresponding to the β-SiC phase become weaker, indicating the decrease in its content in the films. The XRD patterns of the composite films deposited with 0.15 vol% and 0.175 vol% TMS shown in Fig. 7 and 8 reflect the same nature as the composite films deposited with 0.075 vol% TMS discussed above. In these two figures, the composite films deposited with bias currents of 1.5 A and 3.0 A contain diamond, β-SiC and cobalt silicides. The films deposited with bias current of 4.5 A contain mainly diamond. Therefore, with the increase of bias current, the content of diamond increases, while that of β-SiC decreases. These results are in accordance with the EPMA results.

Fig. 9 shows Raman spectra obtained from the diamond/β-SiC/cobalt silicide composite films deposited with 0.075 vol% TMS in the gas phase with only a change in bias current. For the films deposited with bias currents of 0 and 1.5 A, the diamond phonon line (at around 1 332 cm^{-1}) appears to be broadened.

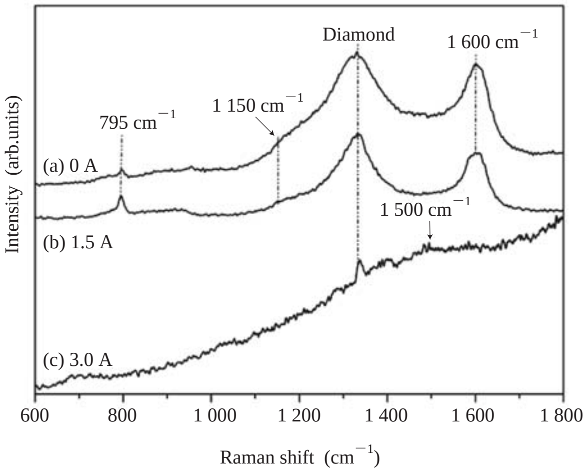

Fig. 9 Raman spectra of the composite films deposited with 0.075 vol% tetramethylsilane in gas phase with bias currents of (a) 0 (sample A1), (b) 1.5 A (sample A2) and (c) 3.0 A (sample A3)

The peak broadening is attributed to the reduction in phonon's lifetime that can be correlated with the concentration of point defects in diamond crystalline[26,27]. Due to the introduction of TMS in gas, there is a competition between the diamond and β-SiC crystallites to occupy the spaces available on the substrates. The presence of TMS does not allow an efficient crystal growth during the deposition. Therefore, there may be a large number of point defects in diamond crystalline. When the bias current is increased to 3.0 A, the diamond peak becomes narrower than the diamond peak in the former two cases, which can be ascribed to a well-crystallized diamond phase[28,29].

Moreover, the narrower diamond peak in Fig. 9(c) can also be attributed to the increase in diamond crystal size. SEM images in Fig. 2 indicate that the grain size of diamond increases with bias current. The peak at around 1 150 cm^{-1} shown by an arrow is observed in the films deposited with bias currents of 0 and 1.5 A. This peak is assigned to the modes associated with the segments of trans-polyacetylene[30]. It is reported that trans-polyacetylene is formed together with nm-sized diamond crystals[31]. Therefore, diamond crystallites in nanometer size may exist in composite films deposited with the bias currents of 0 and 1.5 A. The Raman spectra of films deposited with the bias currents of 0 and 1.5 A show the peak at approximately 1 600 cm^{-1} corresponding to a disorder phase of graphitic carbon[32,33]. This may be caused by the presence of TMS in gas phase, which disturbs the growth of diamond crystals, resulting in the enhanced growth of graphitic carbon. For the film deposited with bias current of 3.0 A, there is not such graphitic carbon peak due to the effect of bias. The peak with broad band near 1 500 cm^{-1} shown by an arrow in Fig. 9(c) is related to the disordered sp^3 carbon[34,35]. Although SEM and XRD results (Fig. 2(d) and 6(c)) indicate only diamond formed in this film, EPMA results show that this film consists of 0.210 mol% Si and 0.005 mol% Co. The disordered sp^3 carbon may be caused by the small amount of Si and Co located at the grain boundaries or other defects. The peak at 795 cm^{-1} in the films deposited with bias currents of 0 and 1.5 A is attributed to the zone-centre transverse optical (TO) phonon of β-SiC[36,37], while there is no β-SiC peak in the film deposited with bias current of 3.0 A. Therefore, with the increase of bias current, the content of diamond increases, and that of β-SiC and graphitic carbon decrease.

The experimental results demonstrate that diamond/β-SiC/cobalt silicide composite films deposited with appropriate bias currents and TMS concentrations in the gas phase are composed of diamond, β-SiC and cobalt silicides (CoSi, Co_2Si). The bias current cannot be too high to deposit the three substances of diamond, β-SiC and cobalt silicides in the composite film.

It is evident that bias plays an important role in the growth of diamond in composite films. With the increase of bias current, the content of diamond increase, and the size of diamond becomes larger. During the biasing process, a DC plasma was formed between the positive substrate and the negative hot filaments. Electrons emitted from filaments are accelerated by electric field and collided with the substrate surface. It is proposed that the electron bombardment enhances the dissociation of hydrogen and hydrocarbons on the substrate surface, resulting in the formation of radicals. The increased radicals on substrate may enhance the grain size, growth rate and the oriented growth of diamond particles[24]. With the increase of bias current, the number of electrons which impinge on the substrate increases and the kinetic energy of electron is greatly enhanced. Thus the dissociation of reactive gases including H_2, CH_4 used as C source and TMS used as Si source on the substrate surface can be largely enhanced. The radicals which are important to diamond and β-SiC are both increased. It is evident in Fig. 4(a) and 4(b) that not only diamond crystallites, but also grain size of β-SiC becomes bigger with a higher bias, suggesting the increase of both C and Si sources. However, the concentration of CH_4 in gas phase is about 6 to 13 times as much as that of TMS (1 vol% CH_4 and 0.075 vol%-0.175 vol% TMS). Hence the mixture activated by DC-plasma HFCVD with higher bias current could provide significantly higher content of C source than Si source. The growth rate of diamond becomes faster than that of β-SiC. The growth of diamond becomes more competitive than that of β-SiC, resulting in the increase of content of diamond in composite films.

The compositional variety of composite films depends on the concentration of decomposed C source and Si source. The effects of bias discussed above indicate that the increase in concentration of C source leads to increase in diamond content in the film. Furthermore, when the TMS concentration in gas phase is slightly increased, the contents of Si sources are largely increased, because the gas mixture activated by plasma could provide Si sources with a higher rate[38]. Then the content of β-SiC is significantly increased with the increase of Si source. Take the films deposited at the constant bias current of 3.0 A with only a change in TMS concentration as an example, the film deposited with 0.075 vol% TMS in gas phase only consists of diamond shown in Fig. 2(d), the film deposited with 0.15 vol% TMS in gas phase contains diamond, β-SiC and Co_2Si shown in Fig. 3(b), and the film deposited with 0.175 vol% TMS in gas phase contains mainly β-SiC shown in Fig. 4(b).

It is also found that the diamond secondary nucleation is enhanced by positive bias. Diamond crystallites about 0.5 μm in size were deposited on the grain boundaries of typical micron size diamond grains shown in Figs. 2(d), 3(b), 3(d) and 4(d). The enhancement of secondary nucleation may be related to the C-containing radicals dissociated by electron bombardment. Samples B3 and C3 which were deposited with bias current of 4.5 A contain mainly diamond in the films. With the decrease of TMS from 0.175 vol% to 0.15 vol% (sample C3 to sample B3), the average diamond grain size seems to be decreased shown from Fig. 4(d) to Fig. 3(d). As the ratio of concentration of CH_4 to TMS in the feeding gas increasing with the decreasing of TMS vol%, the C-containing radicals on substrate surface increase, resulting in the enhancement of diamond secondary nucleation and the decrease of diamond grain size.

As a relation between the growth of cobalt silicides and bias currents cannot be found, bias has little effect on the growth of cobalt silicides. The formation of cobalt silicides can be caused by Co which diffuses from bulk and reacts with Si-containing gaseous species. The SEM images in Figs. 3(b), 3(c) and Figs. 4(b), 4(c) indicate that with the increase of TMS concentration in gas phase, the content of β-SiC increases, while that of cobalt silicides decreases. Two reasons may be ascribed to this phenomenon. First, the film becomes so denser with the increase of nanocrystalline β-SiC that there is not enough time for Co which diffuses from bulk to film surface and reacts with Si-containing gaseous species. Second, the growth rate of β-SiC becomes higher than that of cobalt silicides with the increase of TMS in terms of kinetics, resulting in higher content of β-SiC. Samples A3, B3 and C3 contain mainly diamond crystallites. Little of cobalt silicides exist in these films. The high nucleation density and high growth rate of diamond make the films so dense that Co diffusion from the bulk is prevented. However, cobalt may exist on the interface between film and substrate. For the pure diamond film deposited on WC-Co, Co could still diffuse from bulk to the interface during the deposition. In the case of samples A3, B3 and C3, there are no obvious cobalt silicides in the XRD. Without the blocking effect of cobalt silicides at interface, cobalt diffuses easily from bulk to film surface during deposition, which can influence the structure and quality of diamond coating due to the strong catalytic effect of cobalt[39,40]. Moreover, some pits are visible on the surface of these films deposited with high bias currents. Since the pits are not completely filled during diamond deposition, such morphology will lead to a reduction of the mechanical properties which will likely act as sources of cracks during machining[41]. Thus, the bias current cannot be too high to deposit the composite films. Furthermore, the formation of cobalt silicides may also attribute to the Co which diffuses from bulk and reacts with β-SiC in the film. As Gibbs free energies of CoSi and Co_2Si are lower than that of β-SiC at the deposition temperature[42], cobalt silicides are more thermodynamically stable than SiC. When a thermodynamic equilibrium is achieved, cobalt silicides appear. SEM images in Figs. 3(b) and 3(c) indicate that cobalt silicides are formed on β-SiC clusters in the composite films.

The composite films deposited by HFCVD were compared with that deposited by microwave plasma chemical vapor deposition[20,43]. Nanocrystalline diamond/SiC composite films were synthesized on WC-Co substrate using microwave plasma chemical vapor deposition. Also, cobalt silicides ($CoSi_2$, Co_2Si) were obtained in this composite film. Furthermore, with higher microwave power density, the quality of diamond is higher and grain size becomes larger due to high concentration of atomic hydrogen during deposition. This is similar with our results that the quality of diamond crystalline becomes higher with higher bias current.

4　Conclusions

Diamond/β-SiC/cobalt silicide composite films were deposited on WC-Co substrates by DC-plasma assisted HFCVD using a gas mixture of H_2, CH_4 and TMS. The composite films consist of diamond, β-SiC and cobalt silicides (Co_2Si, CoSi). The structure and composition of the composite films can be controlled by adjusting bias current and TMS concentration in gas phase. The bias current cannot be too high to deposit the three substances of diamond, β-SiC and cobalt silicides. Positive bias enhances the secondary nucleation and the growth of diamond. With the increase of bias current, the grain size of diamond becomes larger, the content of diamond increases, and the content of β-SiC decreases. The dissociation of H_2, CH_4 and TMS are all enhanced by electron bombardment during biasing process. As CH_4 vol% is much higher that TMS vol% in the gas phase, the concentration of produced C sources is much higher than that of Si sources with the increase of bias current, which results in more competitive growth of diamond than the growth of β-SiC. Cobalt silicides were co-existed with β-SiC due to the Co which diffuses from bulk and reacts with β-SiC or Si-containing gaseous species. Finally, the distribution of diamond and β-SiC was manipulated. Different structures and composition can influence the mechanical properties of films and improve the cutting performance of diamond coated cutting tools. In addition, by understanding and controlling the growth of composite thin films, this work is helpful for developing new composite materials and super hard thin films.

Acknowledgments

We would like to thank Dr. Stephan Wang and Mr. Yongneng Xie for correcting the language of the whole paper. This work was supported by Shenzhen Municipality Project (JCYJ20150630114942259), Shenzhen Municipality Science and Technology Planning Project (JSGG20160229202951528, KQJSCX20160301145319, JCYJ20160122143847150), Scientific Equipment Project of Chinese Academy of Sciences (yz201440), Science and Technology Planning Project of Guangdong Province (2014A010105032, 2014A010106016), Natural Science Foundation of Guangdong Province, China (2014A030310482) and Guangdong Innovative and Entrepreneurial Research Team Program (2013C090).

References

[1] Lei X, Shen B, Cheng L, et al. Influence of pretreatment and deposition parameters on the properties and cutting performance of NCD coated PCB micro drills [J]. International Journal of Refractory Metals & Hard Materials, 2014, 43(3): 30-41.

[2] Haubner R, Kalss W. Diamond deposition on hardmetal substrates-comparison of substrate pre-treatments and industrial applications [J]. International Journal of Refractory Metals & Hard Materials, 2010, 28(4): 475-483.

[3] Liu MN, Bian YB, Zheng SJ, et al. Growth and mechanical properties of diamond films on cemented carbide with buffer layers [J]. Thin Solid Films, 2015, 34: 165-169.

[4] Lu P, Gomez H, Xiao X, et al. Coating thickness and interlayer effects on CVD-diamond film adhesion to cobalt-cemented tungsten carbides [J]. Surface & Coatings Technology, 2013, 215(2): 272-279.

[5] Mandal S, Thomas ELH, Jenny TA, et al. Chemical nucleation of diamond films [J]. ACS Applied Materials & Interfaces, 2016, 8(39): 26220-26225.

[6] Park BS, Baik YJ, Lee KR, et al. Behaviour of Co binder phase during diamond deposition on WC-Co substrate [J]. Diamond & Related Materials, 1993, 2(5): 910-917.

[7] Dumpala R, Kumar N, Kumaran CR, et al. Adhesion characteristic of nano- and micro-crystalline diamond coatings: Raman stress mapping of the scratch tracks [J]. Diamond & Related Materials, 2014, 44(4): 71-77.

[8] Cui Y, Wang W, Shen B, et al. A study of CVD diamonjd deposition on cemented carbide ball-end milling tools with high cobalt content using amorphous ceramic interlayers [J]. Diamond & Related Materials, 2015, 59: 21-29.

[9] Hei H, Ma J, Li X, et al. Preparation and performance of chemical vapor deposition diamond coatings synthesized onto the cemented carbide micro-end mills with a SiC interlayer [J]. Surface & Coatings Technology, 2015, 261: 272-277.

[10] Lin CR, Kuo CT, Chan RM. Improvement in adhesion of diamond films on cemented WC substrate with Ti-Si interlayers [J]. Diamond & Related Materials, 1998, 7(11-12): 1628-1632.

[11] Haubner R, Lux B. Diamond deposition on steel substrates using intermediate layers [J]. International Journal of Refractory Metals & Hard Materials, 2006, 24(5): 380-386.

[12] Li YS, Tang Y, Yang Q, et al. Al-enhanced nucleation and adhesion of diamond films on

WC-Co substrates [J]. International Journal of Refractory Metals & Hard Materials, 2008, 26(5): 465-471.

[13] Manaud JP, Poulon A, Gomez S. A comparative study of CrN, ZrN, NbN and TaN layers as cobalt diffusion barriers for CVD diamond deposition on WC-Co tools [J]. Surface & Coatings Technology, 2007, 202(2): 222-231.

[14] Xu F, Xu JH, Yuen MF, et al. Adhesion improvement of diamond coatings on cemented carbide with high cobalt content using PVD interlayer [J]. Diamond & Related Materils, 2013, 34(2): 70-75.

[15] Polini R, Barletta M. On the use of CrN/Cr and CrN interlayers in hot filament chemical vapour deposition (HF-CVD) of diamond films onto WC-Co substrates [J]. Diamond & Related Materils, 2008, 17(3): 325-335.

[16] Qin F, Chou YK, Dohlen D, et al. Coating thickness effects on diamond coated cutting tools [J]. Surface & Coatings Technology, 2009, 204(6-7): 1056-1060.

[17] Xiang L. Zwischenschichten zur entwicklung haftfester CVD-diamantbeschichtungen auf Stahl [D]. TU Braunshweig, 2002.

[18] Wang T, Zhuang H, Jiang X. One step deposition of highly adhesive diamond films on cemented carbide substrates via diamond/β-SiC composite interlayers [J]. Applied Surface Science, 2015, 359: 790-796.

[19] Srikanth VVSS, Hisham SA, Staedler T, et al. Nanocrystalline diamond/β-SiC composite interlayers for the deposition of continuous diamond films on W and Mo substrate [J]. Surface & Coatings Technology, 2007, 201(22): 8981-8985.

[20] Srikanth VVSS, Jiang X, Kopf A. Deposition of diamond/β-SiC nanocomposite films onto a cutting tool material [J]. Surface & Coatings Technology, 2010, 204(15): 2362-2367.

[21] Song BH, Yoon DY. The effect of d.c. glow discharge on hot filament chemical vapor deposition of diamond [J]. Diamond & Related Materils, 2000, 9(1): 82-86.

[22] Dua AK, George VC, Friedrich M, et al. Effect of deposition parameters on different stages of diamond deposition in HFCVD technique [J]. Diamond & Related Materils, 2004, 13(1): 74-84.

[23] Faure C, Teulé-Gay L, Manaud J, et al. Mechanisms of time-modulated polarized nanocrystalline diamond growth [J]. Surface & Coatings Technology, 2013, 222(19): 97-103.

[24] Nose K, Suwa T, Ikejiri K, et al. Ion acceleration in bias-enhanced nucleation of diamond at relatively high pressures [J]. Diamond & Related Materials, 2011, 20(5-6): 687-692.

[25] Peters MG, Cummings RH. Methods for coating adherent diamond films on cemented tungsten carbide substrates: US, US5236740 [P]. 1993-08-17 [2016-10-12].

[26] Morell G, Perez W, Ching-Prado E, et al. Anharmonic interactions in beryllium oxide [J]. Physical Review B, 1996, 53(9): 5388-5395.

[27] Gheeraert E, Deneuville A, Bonnot AM, et al. Defects and stress analysis of the Raman spectrum of diamond films [J]. Bulletin of Toyama Technical College, 1991, 1(5-6): 525-528.

[28] Knight DS, White WB. Characterization of diamond films by Raman spectroscopy [J]. Journal of Materials Research, 1989, 4(2): 385-393.

[29] Nistor LC, Landuyt JV, Ralchenko VG, et al. Nanocrystalline diamond films: transmission electron microscopy and Raman spectroscopy characterization [J]. Diamond & Related Materials, 1997, 6(1): 159-168.

[30] Ferrai AC, Robertson J. Origin of the 1 150 cm^{-1} Raman mode in nanocrystalline diamond [J]. Physical Review B, 2001, 63(12): 263-271.

[31] Lopezrios T, Sandre E, Leclercq S, et al. Polyacetylene in diamond films evidenced by surface enhanced Raman scattering [J]. Physical Review Letters, 1996, 76(26): 4935-4938.

[32] Nemanich RJ, Glass JT, Lucovsky G, et al. Raman scattering characterization of carbon bonding in diamond and diamondlike thin films [J]. Journal of Vacuum Science & Technology A: Vacuum Surfaces & Films, 1988, 6(3): 1783-1787.

[33] Chiang MJ, Hon MH. Positive dc bias-enhanced diamond nucleation with high CH_4 concentration [J]. Diamond & Related Materials, 2001, 10(8): 1470-1476.

[34] Wang WN, Fox NA, May PW, et al. Laser Raman studies of polycrystalline and amorphic diamond films [J]. Physica Status Solidi, 1996, 154(1): 255-268.

[35] Nistor LC, Landuyt Van J, Ralchenko VG, et al. Nanocrystalline diamond films: transmission electron microscopy and Raman spectroscopy characterization [J]. Diamond & Related Materials, 1997, 6(1): 159-168.

[36] Sasaki Y, Nishina Y, Sato M, et al. Raman study of SiC fibres made from polycarbosilane [J]. Journal of Material Science, 1987, 22(2): 443-448.

[37] Olego D, Cardona M. Raman scattering by coupled LO-phonon—plasmon modes and forbidden TO-phonon Raman scattering in heavily doped p-type GaAs [J]. Physical Review B, 1981, 24(12): 7217-7232.

[38] Zhao YL, Zhang RQ, Srikanth VVSS, et al. Possible gas-phase reactions of H_2/CH_4/Tetramethylsilane in diamond/β-SiC nanocomposite film deposition: an Ab-initio study [J]. Journal of Physical Chemistry A, 2007, 111(18): 3554-3559.

[39] Wei QP, Yu ZM, Ashfold MNR, et al. Fretting wear and electrochemical corrosion of well-adhered CVD diamond films deposited on steel substrates with a WC-Co interlayer [J]. Diamond & Related Materials, 2010, 19(10): 1144-1152.

[40] Donnet JB, Paulmier D, Oulanti H, et al. Diffusion of cobalt in diamond films synthesized by combustion flame method [J]. Carbon, 2004, 42(11): 2215-2221.

[41] Wei QP, Yu ZM, Ashfold MNR, et al. Synthesis of micro-or nano-crystalline diamond films on WC-Co substrates with various pretreatments by hot filament chemical vapor deposition [J]. Applied Surface Science, 2010, 256(13): 4357-4364.

[42] Seng WF, Barnes PA. Calculations of cobalt silicide and carbide formation on SiC using the Gibbs free energy [J]. Materials Science Engineering B, 2000, 76(3): 225-231.

[43] Zhuang H, Zhang L, Staedler T, et al. Highly selective diamond and β-SiC crystal formation at increased atomic hydrogen concentration: a route for synthesis of high-quality and patterned hybrid diamond/β-SiC composite film [J]. Scripta Materialia, 2011, 65(6): 548-551.